# Hypernucleus formation in high-energy nuclear collisions

M. Wakai
*Department of Physics, Osaka University, Toyonaka, Osaka 560, Japan*

H. Bandō
*Division of Mathematical Physics, Fukui University, Fukui 910, Japan*

M. Sano
*Institute for Nuclear Study, University of Tokyo, Tanashi, Tokyo 188, Japan*
(Received 11 April 1988)

The hypernucleus formation probability in nuclear collisions is formulated with a coalescence model and is calculated for $p$ + Ne and Ne + Ne collisions at 2.1 GeV/nucleon and 5 GeV/nucleon. It is found that the probability of the hypernucleus formation at 5 GeV/nucleon is about a few times larger than at 2.1 GeV/nucleon and also that the probability of the hypernucleus formation in the Ne + Ne collisions is a few times larger than that in the $p$ + Ne collisions. The cross section of Λ-hypernucleus formation is of the order of μb in the Ne + Ne collisions at 5 GeV/nucleon. The formation probability of multi-Λ hypernucleus is also discussed.

## I. INTRODUCTION

The formation of hypernuclei has been undertaken by proton-, electron-, pion-, and kaon-nucleus collisions. Meanwhile, we have known from the experiments that production cross sections of kaons[1] and Λ particles[2] are considerably large in high-energy heavy-ion collisions even at 2.1 GeV/nucleon. We can expect, therefore, that high-energy heavy-ion collisions become also a possible tool for the formation of a hypernucleus and moreover for the formation of exotic hypernucleus with multi-Λ particles. The possibility of creating hypernuclei in heavy-ion collisions was first suggested by Kerman and Weiss.[3] They obtained a rather unrealistic large amount of formation cross section using a crude model without the momentum distribution of a Λ particle produced by nuclear collisions. However, the formation probability of a hypernucleus depends strongly on the momentum of the Λ particle, since the produced Λ particle has to stay in a nucleus.

The purpose of this paper is to apply the coalescence model[4] to a description of the hypernucleus formation and to estimate cross sections of single and double Λ-hypernucleus formation in nucleus-nucleus collisions and also in proton-nucleus collisions. Asai and two of the present authors (H.B. and M.S.) (Ref. 5) have estimated single Λ-hypernucleus formation cross sections at 2.1 GeV/nucleon with the coalescence model, employing the available experimental and theoretical information on high-energy heavy-ion collisions. The calculations were further extended by the present authors[6] to higher energy of 5 GeV/nucleon, taking account of various possible elementary processes. However, the effect of temporal distributions of a nucleus and a Λ particle, which coalesce with each other, was not considered. In the present work, we formulate the probability of hypernucleus formation based on the coalescence model by using a time-dependent density matrix and estimate the hypernucleus formation cross sections in nuclear collisions at 2.1 and 5 GeV/nucleon.

The basic formulations are presented in Sec. II. The formation cross section of a hypernucleus is expressed by the product of the Λ-particle cross section, the nuclear fragment cross section, and a coalescence factor. We employ reasonable theoretical evaluations for the Λ particle and the nuclear fragment cross sections presented in Secs. III and IV, respectively. In Sec. V the coalescence factor is estimated assuming spatial and temporal distributions of a Λ particle and a nuclear fragment. The results and the discussions are presented in Secs. VI and VII. The final conclusion summarized in Sec. VIII.

## II. FORMATION CROSS SECTION OF HYPERNUCLEUS

We assume that a hypernucleus is formed through the coalescence between a nuclear fragment and a Λ particle proceeded in high-energy nuclear collisions. The probability of emission of the hypernucleus is given by the probability of finding its component in a highly excited many-body system. The probability for finding a particle at a given momentum $\mathbf{k}$ and at time $t$ is given by

$$P_1(\mathbf{k},t)=\frac{1}{(2\pi)^3}\int d\mathbf{r}\,d\mathbf{r}'e^{-i\mathbf{k}\cdot\mathbf{r}}\rho(\mathbf{r};\mathbf{r}',t)e^{i\mathbf{k}\cdot\mathbf{r}'}\ , \qquad (1)$$

where $\rho(\mathbf{r};\mathbf{r}',t)$ is the single-particle density matrix defined by the relation

$$\rho(\mathbf{r};\mathbf{r}',t)=\langle\Psi(t)\,|\,\hat{\psi}^\dagger(\mathbf{r})\hat{\psi}(\mathbf{r}')\,|\,\Psi(t)\rangle\ . \qquad (2)$$

Here $\hat{\psi}^\dagger\mathbf{r}$ and $\hat{\psi}(\mathbf{r})$ are single nucleon creation and destruction operators, and $\Psi(t)$ is the full wave function for the system and is normalized as follows:

 

$$\int \Psi^*(\mathbf{r}_1,\mathbf{r}_2,\ldots,\mathbf{r}_N,t)\Psi(\mathbf{r}_1,\mathbf{r}_2,\ldots,\mathbf{r}_N,t)d\mathbf{r}_1 d\mathbf{r}_2\cdots d\mathbf{r}_N=1 \ . \tag{3}$$

The probability of finding a particle at a momentum $\mathbf{k}$ is obtained by taking a limit of the time variable.

$$P_1(\mathbf{k})=\lim_{t\to\infty} P_1(\mathbf{k},t)=\frac{1}{(2\pi)^3}\int_{-\infty}^{\infty} dt\int d\mathbf{r}\,d\mathbf{r}' e^{-i\mathbf{k}\cdot\mathbf{r}}\dot{\rho}(\mathbf{r};\mathbf{r}',t)e^{i\mathbf{k}\cdot\mathbf{r}'} \ , \tag{4}$$

where $\dot{\rho}(\mathbf{r};\mathbf{r}',t)$ expresses the time derivative of the single-particle density matrix.[7–9] The expression (4) can be generalized to the case of emission of two particles moving with momenta $\mathbf{k}_1$ and $\mathbf{k}_2$ and the probability is expressed with the two-particle density matrix $\rho(\mathbf{r}_1,\mathbf{r}_2;\mathbf{r}_1',\mathbf{r}_2',t)$ as

$$\begin{aligned}P_2(\mathbf{k}_1,\mathbf{k}_2)&=\lim_{t\to\infty} P_2(\mathbf{k}_1,\mathbf{k}_2,t)\\&=\frac{1}{(2\pi)^3}\int_{-\infty}^{\infty} dt\int d\mathbf{r}_1 d\mathbf{r}_2 d\mathbf{r}_1' d\mathbf{r}_2'\Phi^*_{\mathbf{k}_1\mathbf{k}_2}(\mathbf{r}_1,\mathbf{r}_2)\dot{\rho}(\mathbf{r}_1,\mathbf{r}_2;\mathbf{r}_1',\mathbf{r}_2',t)\Phi_{\mathbf{k}_1\mathbf{k}_2}(\mathbf{r}_1',\mathbf{r}_2') \ .\end{aligned} \tag{5}$$

In the case of hypernucleus formation, the wave function $\Phi$ can be factorized into wave functions of center of mass and relative motions, and the relative wave function $\psi(\mathbf{r})$ is described as bound states of a nuclear fragment and a $\Lambda$ particle. Equation (5) is then rewritten as

$$P_2^{(\Lambda F)}(\mathbf{K})=\frac{w(\Lambda F)}{(2\pi)^3}\int_{-\infty}^{\infty} dt\int d\mathbf{r}_1 d\mathbf{r}_2 d\mathbf{r}_1' d\mathbf{r}_2' \exp(-i\mathbf{K}\cdot\mathbf{R})\psi^*(\mathbf{r})\dot{\rho}(\mathbf{r}_1,\mathbf{r}_2;\mathbf{r}_1',\mathbf{r}_2',t)\exp(i\mathbf{K}\cdot\mathbf{R}')\psi(\mathbf{r}') \ , \tag{6}$$

where $\mathbf{r}=\mathbf{r}_1-\mathbf{r}_2$, $\mathbf{R}=(M_\Lambda\mathbf{r}_1+M_F\mathbf{r}_2)/(M_\Lambda+M_F)$, $\mathbf{K}=\mathbf{k}_1+\mathbf{k}_2$, with $\mathbf{k}_1$ and $\mathbf{k}_2$ being conjugate to $\mathbf{r}_1$ (for $\Lambda$ particle) and $\mathbf{r}_2$ (for nuclear fragment), $M_\Lambda$ and $M_F$ are masses of the $\Lambda$ particle and the nuclear fragment $F$, respectively, and $w(\Lambda F)$ is a statistical weight factor due to spins.

We assume that the two-particle density matrix in Eq. (6) is approximately given by a simple product of two one-particle density matrices $\rho^{(\Lambda)}$ and $\rho^{(F)}$, i.e.,

$$\rho^{(\Lambda F)}(\mathbf{r}_1,\mathbf{r}_2;\mathbf{r}_1',\mathbf{r}_2',t)\simeq\rho^{(\Lambda)}(\mathbf{r}_1;\mathbf{r}_1',t)\rho^{(F)}(\mathbf{r}_2;\mathbf{r}_2',t) \ , \tag{7}$$

which implies that the correlation between the $\Lambda$ particle and the nuclear fragment $F$ is negligible. We further assume that the one-particle density matrix, for instance, $\rho^{(\Lambda)}$, can be written as

$$\begin{aligned}&\rho^{(\Lambda)}(\mathbf{r}_1;\mathbf{r}_1',t)\\&\quad=D^{(\Lambda)}\left[\frac{\mathbf{r}_1+\mathbf{r}_1'}{2},t\right]\int d\mathbf{k}_1 \exp[i\mathbf{k}_1\cdot(\mathbf{r}_1-\mathbf{r}_1')]P_1^{(\Lambda)}(\mathbf{k}_1) \ .\end{aligned} \tag{8}$$

Here $D$ describes the spatial and temporal distributions of the $\Lambda$ particle and is normalized to unity as

$$\lim_{t\to\infty}\int d\mathbf{r}\,D(\mathbf{r},t)=\int_{-\infty}^{\infty} dt\int d\mathbf{r}\,\dot{D}(\mathbf{r},t)=1 \ . \tag{9}$$

Thus we can obtain the expression for the probability of hypernucleus formation as

$$P_2^{(\Lambda F)}(\mathbf{K})=\int d\mathbf{k}\,F_2(\mathbf{k})P_1^{(\Lambda)}(\mathbf{k}_1+\mathbf{k})P_1^{(F)}(\mathbf{k}_2-\mathbf{k}) \ , \tag{10}$$

where $\mathbf{k}_1=M_\Lambda\mathbf{K}/(M_\Lambda+M_F)$ and $\mathbf{k}_2=M_F\mathbf{K}/(M_\Lambda+M_F)$. The function $F_2$ is defined by

$$\begin{aligned}F_2(\mathbf{k})=w(\Lambda F)\int_{-\infty}^{\infty} dt\int d\mathbf{q}\frac{\partial}{\partial t}[\tilde{D}^{(\Lambda)}(\mathbf{q},t)\tilde{D}^{(F)}(-\mathbf{q},t)]\\\times\tilde{\psi}^*(\mathbf{k}+\tfrac{1}{2}\mathbf{q})\tilde{\psi}(\mathbf{k}-\tfrac{1}{2}\mathbf{q}) \ ,\end{aligned} \tag{11}$$

where $\tilde{\psi}$ and $\tilde{D}$ are Fourier transforms of $\psi$ and $D$, respectively.

The extension of the spatial distribution of the source matter, $D(\mathbf{r},t)$, is much larger than that of the $(\Lambda F)$ bound system, $\psi(\mathbf{r})$. In momentum space, the extension of $\tilde{D}(\mathbf{q},t)$ is smaller than that of $\tilde{\psi}(\mathbf{q})$. In Eq. (11), therefore, the extension of $F_2(\mathbf{k})$ is of the same order of magnitude as that of $\tilde{\psi}^*\tilde{\psi}$. When $P_1^{(\Lambda)}P_1^{(F)}$ varies slowly within the extension of $F_2(\mathbf{k})$, we can approximately write

$$P_1^{(\Lambda)}(\mathbf{k}_1+\mathbf{k})P_1^{(F)}(\mathbf{k}_2-\mathbf{k})\simeq g_{\Lambda F}(\mathbf{k})P_1^{(\Lambda)}(\mathbf{k}_1)P_1^{(F)}(\mathbf{k}_2) \ . \tag{12}$$

Then expression (10) becomes

$$P_2^{(\Lambda F)}(\mathbf{K})=S_{\Lambda F}P_1^{(\Lambda)}(\mathbf{k}_1)P_1^{(F)}(\mathbf{k}_2) \ , \tag{13}$$

where $S_{\Lambda F}$ is the coalescence factor defined by

$$S_{\Lambda F}=\int d\mathbf{k}\,F_2(\mathbf{k})g_{\Lambda F}(\mathbf{k}) \ . \tag{14}$$

The effect of temporal distribution of the $\Lambda$-particle and the nuclear fragment $F$ is included in the coalescence factor $S_{\Lambda F}$ through the function $F_2(\mathbf{k})$ given by Eq. (11). (See Fig. 1).

The probabilities $P^{(i)}(\mathbf{k})$ in Eq. (13) are related to the corresponding cross sections as $P^{(i)}(\mathbf{k})=(\gamma_i/\sigma_r)d^3\sigma^{(i)}/dk^3$ ($i=\Lambda,F$), where $\gamma_i=(M_i^2+\mathbf{k}^2)^{1/2}/M_i$ is the Lorentz factor and $\sigma_r$ is the reaction cross section. Therefore, the formation cross section of a hypernucleus is expressed by

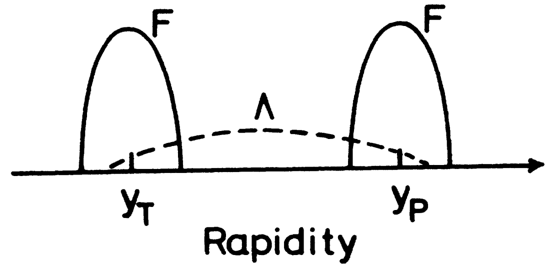


FIG. 1. Schematic picture of rapidity distribution of $\Lambda$ particle and nuclear fragment $F$.

the product of the Λ-particle and nuclear fragment $F$ cross sections, and is given by using the momentum $\mathbf{k}_c$ per particle $[\mathbf{k}_c=\mathbf{K}/(m_\Lambda+m_F)]$ as follows:

$$\frac{\gamma}{\sigma_r}\frac{d^3\sigma^{(\Lambda F)}}{dk_c^2} = \left[\frac{m_\Lambda+m_F}{m_\Lambda m_F}\right]^3 S_{\Lambda F}\left[\frac{\gamma}{\sigma_r}\frac{d^3\sigma^{(\Lambda)}}{dk_c^3}\right]\left[\frac{\gamma}{\sigma_r}\frac{d^3\sigma^{(F)}}{dk_c^3}\right], \tag{15}$$

where $m_\Lambda=M_\Lambda/M_n$, $m_F=M_F/M_n$, $\gamma=[1+(k_c/M_n)^2]^{1/2}$, and $M_n$ is the nucleon mass.

Following the procedure mentioned above, we can also obtain a general expression for the formation cross section of a $n\Lambda$ hypernucleus such that

$$\frac{\gamma}{\sigma_r}\frac{d^3\sigma^{(n\Lambda,F)}}{dk_c^3} = \left[\frac{nm_\Lambda+m_F}{m_\Lambda^n m_F}\right]^3 S_{n\Lambda,F}\left[\frac{\gamma}{\sigma_r}\frac{d^3\sigma^{(\Lambda)}}{dk_c^3}\right]^n \times\left[\frac{\gamma}{\sigma_r}\frac{d^3\sigma^{(F)}}{dk_c^3}\right]. \tag{16}$$

An explicit expression of the coalescence factor $S_{n\Lambda,F}$ will be given in Sec. V for the case of a double-Λ hypernucleus $(n=2)$ together with that of a single-Λ hypernucleus $(n=1)$.

Thus if we had sufficient experimental data of the Λ-particle and nuclear fragment $F$ production cross sections, we would calculate the formation probabilities with Eq. (16). However, due to the lack of experimental information, we employ reasonable theoretical evaluation of the Λ particle and the nuclear fragment production cross sections and the coalescence factor discussed in Secs. III, IV, and V.

## III. INCLUSIVE CROSS SECTIONS OF Λ PARTICLES

Inclusive kaon and Λ-particle cross sections have been measured at 2.1 GeV/nucleon for several projectile-target combinations. In the 2.1 GeV/nucleon beam energy range, the possible types of particle production process are limited to

$$N+N\rightarrow N+N+\alpha\pi \quad (\alpha=0,1,2,\dots) \tag{17a}$$

$$\searrow N+Y+K, \tag{17b}$$

where $Y$ denotes a hyperon (Λ or Σ particle). In conjunction with the experiments, theoretical studies have been made by many authors. According to the statistical phase-space model,[10,11] the inclusive cross section of a particle emitted with the momentum $p$ is written as

$$E\frac{d^3\sigma}{dp^3}=\sum_{MN}\sigma_{AB}(M,N)\mathcal{J}_{MN}(\mathbf{p}). \tag{18}$$

Here $A$ and $B$ denote the projectile and target nuclei, and $\sigma_{AB}(M,N)$ specifies the cross section for a subprocess in which $M$ projectile nucleons interact with $N$ target nucleons. The function $\mathcal{J}_{MN}(\mathbf{p})$ denotes the momentum distribution of the observed particles emitted in the subprocess $(M,N)$.

The cross section $\sigma_{AB}(M,N)$ is factorized into the respective nucleon-nucleus cross section in the straight-line geometry.

$$\sigma_{AB}(M,N)=\sigma_A(M)\sigma_B(N)/\sigma_{NN}, \tag{19}$$

where

$$\sigma_A(M)=\frac{1}{M!}\int d^2s[\overline{M}_A(\mathbf{s})]^M\exp[-\overline{M}_A(\mathbf{s})],$$

$$\overline{M}_A(\mathbf{s})=\sigma_{NN}\int dz\,\rho_A(\mathbf{s},z).$$

Here $\rho_A(\mathbf{s},z)$ denotes the nuclear density distribution and $\sigma_{NN}$ is the total $N$-$N$ cross section which is taken to be 40 mb.

The momentum distribution $\mathcal{J}_{MN}(\mathbf{p})$ is given as follows:

$$\mathcal{J}_{MN}(\mathbf{p})=\sum_i n_i\mathcal{P}_{MN}(n_i)\Phi_L(\mathbf{p}). \tag{20}$$

The probability $\mathcal{P}_{MN}(n_i)$ for producing $n_\pi$ pions, $n_\Lambda$ lambdas, and $n_\Sigma$ sigmas in the subprocess $(M,N)$ involving $\nu NN$ collisions is given by

$$\mathcal{P}_{MN}(n_\pi,n_\Lambda,n_\Sigma) =\frac{\nu}{MN}\sum_{j_0=1}^{\nu}\sum_{j_1=0}^{\nu}\cdots\sum_{j_\beta=0}^{\nu}\frac{\nu!}{\prod_{\alpha=0}^{\beta}j_\alpha!n_\Lambda!n_\Sigma!}\prod_{\alpha=0}^{\beta}[q_\pi(\alpha)]^{j_\alpha}q_\Lambda^{n_\Lambda}q_\Sigma^{n_\Sigma}\delta\left[\nu-n_\Lambda-n_\Sigma-\sum_{\alpha=0}^{\beta}j_\alpha\right] \times\delta\left[n_\pi-\sum_{\alpha=1}^{\beta}\alpha j_\alpha\right]\theta(M+N-n_\Lambda-n_\Sigma)+\frac{MN-\nu}{MN}\delta_{n_\pi 0}\delta_{n_\Lambda 0}\delta_{n_\Sigma 0}. \tag{21}$$

In Eq. (21), the $q_i$ are the branching ratios for the respective processes given by Eq. (17). The normalized momentum distribution $\Phi_L(\mathbf{p})$ of the respective products is

$$\Phi_L(\mathbf{p}_1)=\int\prod_{j=2}^{L}\frac{d^3p_j}{E_j}\delta^3\left[\prod_{j=1}^{L}\mathbf{p}_j-\mathbf{P}_{MN}\right]\delta\left[\sum_{j=1}^{L}E_j-E_{MN}\right]\Big/\int\prod_{j=1}^{L}\frac{d^3p_j}{E_j}\delta^3\left[\prod_{j=1}^{L}\mathbf{p}_j-\mathbf{P}_{MN}\right]\delta\left[\sum_{j=1}^{L}E_j-E_{MN}\right]. \tag{22}$$

The subscript $L$ denotes a set of $M+N-n_\Lambda-n_\Sigma$ nucleons, $n_\Lambda$ lambdas, $n_\Sigma$ sigmas, $n_\pi$ pions, and $n_\Lambda+n_\Sigma$ kaons.

At the energy of about 5 GeV/nucleon, the following elementary reaction channels should be taken into account in addition to those in Eq. (17):

$$N+N \to N+Y+K+n\pi \quad (n=1,2,\ldots) \tag{23a}$$

$$\searrow N+N+K+\bar{K} \; . \tag{23b}$$

We neglect various hyperon production processes such as $\pi+N \to Y+K$ induced by the secondary particles because the probability for those processes is considered to be very small compared with the branching ratios of the processes in Eqs. (17) and (23).

The set of branching ratios, $q_\pi(\alpha)$, for the process (17a) is taken from empirical formulas fitted to the experimental data of $N$-$N$ scattering up to 5∼6 GeV, that is, $q_\pi(0)=0.354$, $q_\pi(1)=0.412$, $q_\pi(2)=0.192$, and $q_\pi(3)=0.046$ at 2.1 GeV; and $q_\pi(0)=0.350$, $q_\pi(1)=0.228$, $q_\pi(2)=0.215$, and $q_\pi(3)=0.207$ at 5 GeV. The isospin-averaged cross section for the combined process of $N+N \to N+\Lambda+K$ and $N+N \to N+\Sigma+K$ in Eq. (17b) is given by

$$\bar{\sigma}(N+N \to N+Y+K)=0.144 p_{\max}(K)/m_K(\text{mb})$$

(Ref. 12) where $p_{\max}(K)$ is the momentum of the produced kaon at maximum energy in the center-of-mass system. The isospin-averaged cross section for the process (23a) is also given by

$$\bar{\sigma}(N+N \to N+\Lambda+K+\pi)=0.898 p_{\max}(K)/m_K(\text{mb}) \; .$$

The cross section for the kaon pair production (23b), in the energy range of interest, are rather sparse. We use a simple linear parametrization of the cross section

$$\bar{\sigma}(N+N \to N+N+K+\bar{K})=0.0175 p_{\max}(K)/m_K(\text{mb}) \; .$$

The effect of the nuclear Fermi motion on the $\mathcal{J}_{MN}(\mathbf{p})$ is taken into account by using the Fermi-averaged branching ratios for the particle production processes (17) and (23), for instance, defined as follows:

$$\tilde{q}_\Lambda(\alpha)=\frac{1}{\sigma_{NN}}\int\int d^3p_A d^3p_B f(\mathbf{p}_A)f(\mathbf{p}_B) \times\bar{\sigma}(N+N \to N+\Lambda+K+\alpha\pi) \; . \tag{24}$$

The functions $f(\mathbf{p}_A)$ and $f(\mathbf{p}_B)$ describe the Fermi momentum distributions of the nucleon in projectile $A$ and in target $B$, respectively.

The calculated $K^+$ cross sections in the case of Ne-Ne collisions at 2.1 GeV/nucleon are shown in Fig. 2(a) and compared with the experiment.[1] Figures 2(b) and 2(c) give the calculated $\Lambda$-particle cross sections at 2.1 and 5 GeV/nucleon, respectively. In Fig. 3(a) the calculated $K^+$ cross sections in the case of $p$-Ne collisions at 2.1 GeV are shown and compared with the experiment. Figures 3(b) and 3(c) represent the calculated $\Lambda$-particle cross sections at 2.1 and 5 GeV, respectively.

## IV. CROSS SECTIONS OF NUCLEAR FRAGMENTS

The main production of nuclear fragments comes from peripheral heavy-ion collisions. The nuclear fragments show typical factorization of cross sections into a target and a projectile, typical momentum distributions and isotope production ratios.[13] In the projectile rest frame for projectile fragmentations (or in the target rest frame for target fragmentations), a fragment has the form of a Gaussian distribution in momentum space, $\exp(-p^2/2\sigma^2)$ where $\sigma^2$ is the dispersion about the mean and is given by $\sigma_0^2 A_F(A_P-A_F)/(A_P-1)$ with the projectile and fragment mass number $A_P$ and $A_F$. The value of $\sigma_0$ is related to the Fermi momentum of nucleons as $\sigma_0^2=p_f^2/5$. An alternative interpretation for the limiting value of $\sigma$ comes from the antithetical statistical model, in which the fragments are emitted from a source at an excitation energy determined by a temperature $T$ and $\sigma^2$ is given by $TM_n A_F(A_P-A_F)/A_P$. Additional support for the thermal interpretation of a limiting temperature comes from the observation that isotope production cross sections are explained by the statistical formula $\exp(Q_{gg}^{(F)}/T)$ where $Q_{gg}^{(F)}$ are the threshold $Q$ values of the various breakup channels of the projectile into the observed fragments. The agreement between the values of $T$ deduced from the momentum and isotope distributions could be regarded as strong evidence in favor of the thermal interpretation. In the case of target fragmentations, $A_P$ in the expressions mentioned above should be replaced by $A_T$.

In the rest frame of the projectile (or the target), the cross section is given in the nonrelativistic approximation by

$$\frac{d^3\sigma^{(F)}}{dp^3}=\frac{\sigma_c}{4\pi}p\exp\left[\frac{Q_{gg}^{(F)}}{T}-\frac{p^2}{2\mu_F T}\right] \Bigg/ \left[2\mu_F T^2\sum_i \mu_i \exp\left[\frac{Q_{gg}^{(i)}}{T}\right]\right] , \tag{25}$$

where $\mu_F=M_n A_F(A_P-A_F)/A_P$ and $\sigma_c=\pi r_0^2(A_P^{1/3}+A_T^{1/3}-\delta)^2$ with $\delta=1.6$. In Fig. 4 the calculated results of the isotope yield in $^{16}$O+ nucleus collisions at 2.1 GeV/nucleon are shown and compared with the experiment. It is seen that the behavior of relative yield as a function of $Q_{gg}$ is well reproduced with the temperature $T=8$ MeV. We will also apply Eq. (25) to target fragmentations induced by proton beams.

## V. COALESCENCE FACTORS

Here, we have to show how to estimate the coalescence factor. The coalescence factor $S_{\Lambda F}$ includes terms corre-

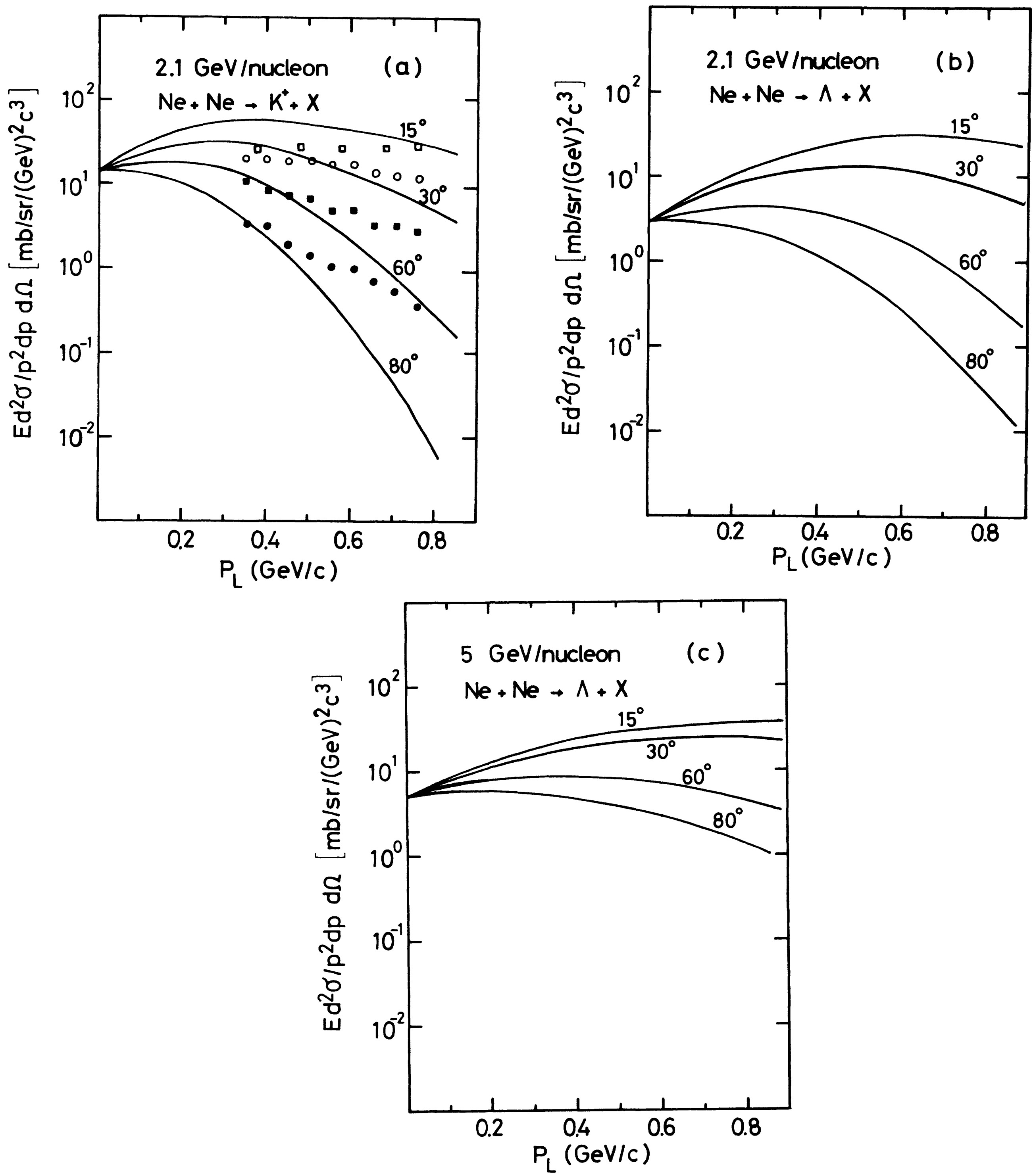


FIG. 2. $K^+$ and $\Lambda$ energy spectra in Ne + Ne collisions at 2.1 and 5 GeV/nucleon. The solid lines represent the cross sections calculated with $\nu = MN$.

sponding to the spatial and temporal distributions as shown in Eqs. (11) and (14). We first consider only an effect of the spatial distribution of a $\Lambda$ particle and a nuclear fragment $F$ on the coalescence factor assuming the time independency of $D(\mathbf{r},t)$. In Sec. V B, we discuss effects of the temporal distribution.

### A. Effects of spatial distribution

In the limit of neglecting the effect of the temporal distribution, the single-particle density matrix in Eq. (1) should be independent of time, that is, $\rho(\mathbf{r};\mathbf{r}',t=0)$ and

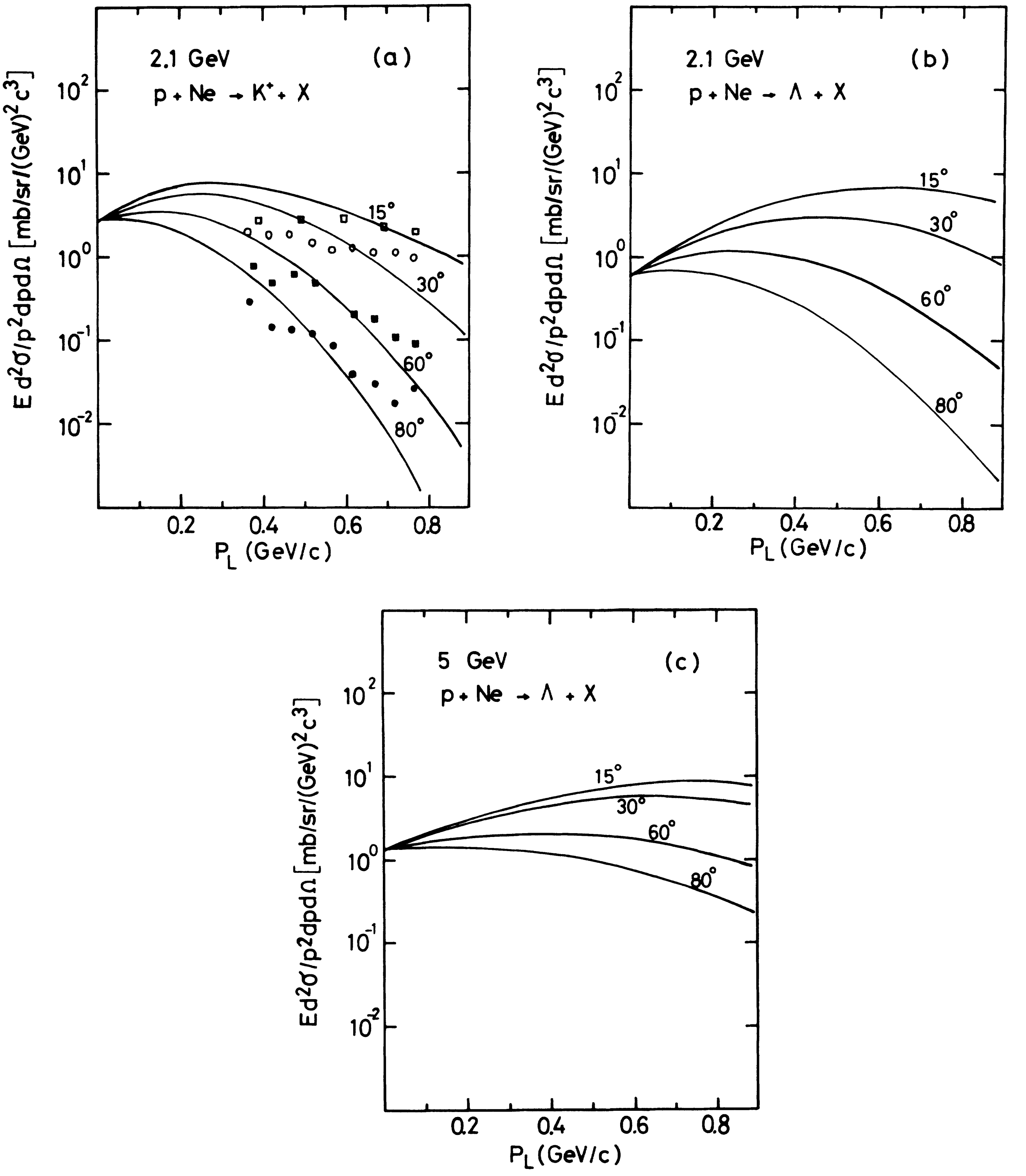


FIG. 3. $K^+$ and $\Lambda$ energy spectra in $p+\mathrm{Ne}$ collisions at 2.1 and 5 GeV. The solid lines represent the cross sections calculated with $\nu = MN$.

the probability for finding a particle at a given momentum $\mathbf{k}$ is given by $P_1(\mathbf{k},t=0)$. Similarly the probability of hypernucleus formation at a momentum $\mathbf{K}$ is given by $P_2^{(\Lambda F)}(\mathbf{K},t=0)$ and then the function $F_2(\mathbf{k})$ in Eq. (10) should be $F_2(\mathbf{k},t=0)$ defined as

$$F_2(\mathbf{k},t=0) = w(\Lambda F) \times \int d\mathbf{q}\, \tilde{D}^{(\Lambda)}(\mathbf{q})\tilde{D}^{(F)}(-\mathbf{q})\tilde{\psi}^*(\mathbf{k}+\tfrac{1}{2}\mathbf{q})\tilde{\psi}(\mathbf{k}-\tfrac{1}{2}\mathbf{q}) \; . \tag{26}$$

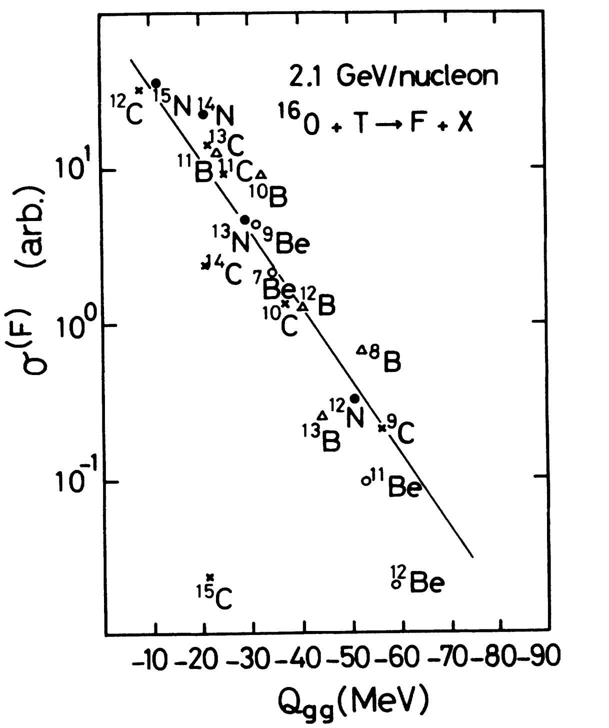


FIG. 4. The relative isotope yield produced by $^{16}$O projectile fragmentation. The solid line corresponds to the cross sections calculated with the temperature $T=8$ MeV.

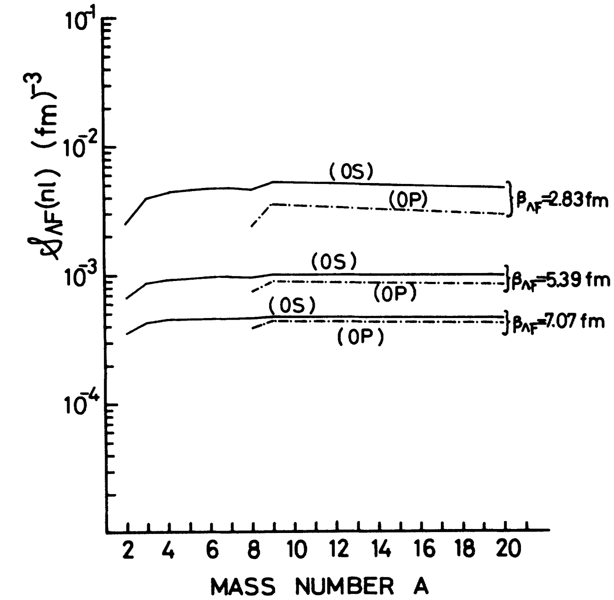


FIG. 5. Coalescence factor $\mathcal{S}_{\Lambda F}(nl)$ plotted as a function of atomic mass number of hypernucleus.

The function $\tilde{g}_{\Lambda F}$ in Eq. (14) may be taken as $\tilde{g}_{\Lambda F}(\mathbf{k})=1$ for the case of weak $\mathbf{k}$ dependence of $P_1$. Then we have

$$S_{\Lambda F}=w(\Lambda F)(2\pi)^3\int d\mathbf{r}\,|\psi(\mathbf{r})|^2\xi_{\Lambda F}(\mathbf{r})\ , \tag{27}$$

where

$$\xi_{\Lambda F}(\mathbf{r})=\int d\mathbf{r}' D^{(\Lambda)}(\mathbf{r}+\mathbf{r}')D^{(F)}(\mathbf{r}')\ . \tag{28}$$

Assuming the harmonic oscillator wave function $\psi_{nlm_s}(\mathbf{r})$ for the $\Lambda$ particle in the hypernucleus and a Gaussian form for the spatial extent $D(\mathbf{r})$, i.e.,

$$D^{(i)}(\mathbf{r})=(\sqrt{\pi}\beta_i)^{-3}\exp[-(r/\beta_i)^2](i=\Lambda \text{ or } F)\ , \tag{29}$$

we obtain the expression

$$S_{\Lambda F}=(2\pi)^3\sum_{nl}(2l+1)\mathcal{S}_{\Lambda F}(nl) \tag{30a}$$

from Eq. (27). The sum runs over bound states of $\Lambda$ particle moving in a potential well with depth of about 30 MeV (i.e., the states having higher energy than 30 MeV are unbound). $\mathcal{S}_{\Lambda F}(nl)$ is given by

$$\mathcal{S}_{\Lambda F}(nl)=\begin{cases}(\sqrt{\pi}\alpha)^{-3} & \text{for } 0s \text{ state}\\ (\sqrt{\pi}\alpha)^{-3}(\beta_{\Lambda F}/\alpha)^2 & \text{for } 0p \text{ state}\ ,\end{cases} \tag{30b}$$

where $\alpha=(b_\Lambda^2+\beta_{\Lambda F}^2)^{1/2}$, $\beta_{\Lambda F}=(\beta_\Lambda^2+\beta_F^2)^{1/2}$, and $b_\Lambda$ is the harmonic oscillator size parameter given by $[(\hbar^2/M_\Lambda)/\hbar\omega_\Lambda]^{1/2}$. In the numerical calculations, we employ a parameter value of $b_\Lambda$ associated with the frequency $\hbar\omega_\Lambda=30A^{-1/3}$ MeV. For the potential depth of 30 MeV, only the $0s$ level becomes a bound state for light nuclei with mass number less than $A=8$, and two levels of $0s$ and $0p$ orbits become bound states for $8\le A\lesssim 20$. The calculated values of $\mathcal{S}_{\Lambda F}(nl)$ are plotted as a function of the hyperfragment mass number in Fig. 5. The results depend on the choice of $\beta_{\Lambda F}$ which represents the extent of the spatial distribution of the source matter and decreases with increase of $\beta_{\Lambda F}$. In the case of weak momentum dependence of $P_1$, the coalescence factor in a double $\Lambda$-hypernucleus formation is given by

$$S_{2\Lambda,F}=w(2\Lambda,F)(2\pi)^6\int d\mathbf{r}\,d\mathbf{R}\,|\psi(\mathbf{r},\mathbf{R})|^2\xi_{2\Lambda,F}(\mathbf{r},\mathbf{R})\ , \tag{31a}$$

where

$$\xi_{2\Lambda,F}(\mathbf{r},\mathbf{R})=\int d\mathbf{x}\,D^{(\Lambda)}(\mathbf{x}+\mathbf{R}+\tfrac{1}{2}\mathbf{r})D^{(\Lambda)}(\mathbf{x}+\mathbf{R}-\tfrac{1}{2}\mathbf{r})D^{(F)}(\mathbf{x})\ . \tag{31b}$$

The coordinate $\mathbf{r}$ represents the relative coordinate between two $\Lambda$ particles and $\mathbf{R}$ is the one between the center of mass of two $\Lambda$ particles and the nuclear fragment $F$. Assuming the properly antisymmetrized harmonic-oscillator wave functions for the $\Lambda$ particles in the hypernucleus and a Gaussian form for the spatial extent $D$, Eq. (31a) is readily evaluated. For example, the contribution of the $(0s)^{2\Lambda}$ configuration is given by

$$S_{2\Lambda,f}=\tfrac{1}{4}(2\pi)^6(\sqrt{\pi}\alpha)^{-3}(\sqrt{\pi}\Gamma)^{-3}\ , \tag{32}$$

where $\alpha=(b_r^2+2\beta_\Lambda^2)^{1/2}$, $\Gamma=(b_R^2+\tfrac{1}{2}\beta_\Lambda^2+\beta_F^2)^{1/2}$, $b_r$ and $b_R$ are the harmonic oscillator size parameters corresponding to the coordinates $\mathbf{r}$ and $\mathbf{R}$, respectively. A general formula of the coalescence factor for the double Λ-hypernucleus formation is given in the Appendix.

### B. Effects of temporal distribution

The density of produced particle is related to space-time quantities. However, we have so far assumed that a hot spot formed in the collision of two identical nuclei stays at the origin of the center-of-mass frame and emits Λ particles immediately after its formation. The overlapping part of two identical nuclei, however, changes time dependently. Therefore, the emission of two Λ particles is also time dependent. Then, to estimate the effect on coalescence factors, we take a simple assumption on the time dependence of $D^{(\Lambda)}$ as follows:

$$\frac{\partial}{\partial t}D^{(\Lambda)}(\mathbf{r},t) = (\sqrt{\pi}\beta_t)^{-1}(\sqrt{\pi}\beta_\Lambda)^{-3}e^{-(\mathbf{r}-\mathbf{v}t)^2/\beta_\Lambda^2}e^{-t^2/\beta_t^2} . \qquad (33a)$$

Here $\mathbf{v}$ denotes the velocity of the hot spot where two identical nuclei overlapped during the collisions, which is assumed to be constant and parallel to the beam direction, and $\beta_t$ is the dispersion of the emission time of the Λ particle. For simplicity, we first ignore the time dependence of $D^{(F)}$ in the following discussion, in order to estimate the order of magnitude of the time dependence of $D^{(\Lambda)}$. By integrating Eq. (33a) and by taking $t=\infty$, we get the expressions for $S_{\Lambda F}$ as follows:

$$S_{\Lambda F}=(2\pi)^3\sum_{nl}(2l+1)\mathcal{S}'_{\Lambda F} , \qquad (33b)$$

where

$$\mathcal{S}'_{\Lambda F}(0s)=\mathcal{S}_{\Lambda F}(0s)(1+v^2\beta_t^2/\alpha^2)^{-1/2} ,$$
$$\mathcal{S}'_{\Lambda F}(0p)=\mathcal{S}_{\Lambda F}(0p)(1+v^2\beta_t^2/\alpha^2)^{-1/2} \times\left[1+\frac{1}{3}\frac{v^2\beta_t^2 b_\Lambda^2}{\beta_{\Lambda F}^2(\alpha^2+v^2\beta_t^2)}\right] . \qquad (33c)$$

$\mathcal{S}_{\Lambda F}(nl)$ is given by Eq. (30c). The reduction factors seen in Eq. (33c) come from the distortion of $D^{(\Lambda)}$ from the spherical distribution, which makes the overlap between the fragment and the Λ particle smaller. It seems to be not unrealistic to assume that the hot spot finishes the emission of Λ particles before the separation from the spectators. The above assumption leads to an estimation of $v\beta_t \simeq R$, where $R$ is the radius of the target (or the projectile).

With the values $\beta_{\Lambda F}\simeq 5.39$ fm, $b_\Lambda \simeq 1.1A^{1/6}$ fm, $R\simeq 3.5$ fm (in the case of the Ne + Ne collision), we get the reduction factors of about 0.5.

Even if we taken into account the time dependence of $D^{(F)}$, the coalescence factor between fragments and Λ particles is not reduced, because the direction of the distortion of $D^{(F)}$ is the same as that of $D^{(\Lambda)}$. Nuclear fragments are produced mainly as a result of the decomposition of the projectile (or the target) at peripheral collisions. Since the center of mass of the fragment system may stay rest in the projectile (or the target) rest frame after the collisions, emissions of the fragments are isotropical with keeping Eq. (29) as a good approximation for the expression of $\lim_{t\to\infty}D^{(F)}(\mathbf{r},t)$.

## VI. RESULTS

Figure 6 shows the formation cross sections of hypernuclei in Ne + Ne collisions, obtained by using Eqs. (18), (25), and (30) for the right-hand side of Eq. (15). Here we

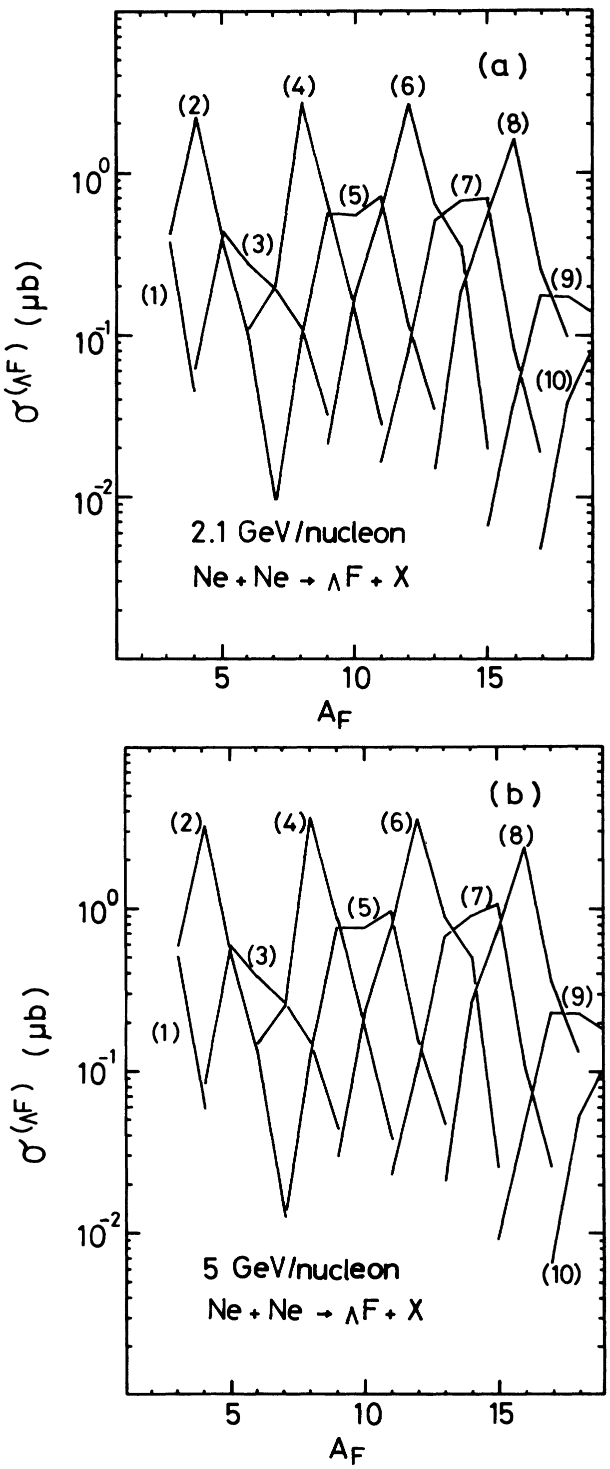


FIG. 6. The hypernucleus formation cross sections in Ne + Ne collisions at 2.1 and 5 GeV/nucleon as a function of nuclear fragment mass number $A_F$. The number on the inside of parentheses indicates an atomic number.

take the parameter value of $\beta_{\Lambda F}=5.39$ fm which comes from the choice $\beta_{\Lambda}=\beta_F$ ($=3.81$ fm). This value corresponds to the extent of the normal compound nucleus consisting of the projectile and target nucleons. In the case of $\beta_{\Lambda F}=7.0$ fm, the calculated cross sections reduce to about half of the magnitudes shown in Fig. 6. It is seen that the formation cross sections in Ne + Ne collisions at 5 GeV/nucleon [Fig. 6(b)] become a few times larger than those at 2.1 GeV/nucleon [Fig. 6(a)] because of the increasing elementary Λ production rates. The results predict appreciable amount of cross sections, although these are smaller than the values predicted by Kerman and Weiss.[3]

The hypernucleus production cross sections in $p$ +Ne collisions are shown in Figs. 7(a) and 7(b) for 2.1 and 5 GeV, respectively. The production cross section in nucleus+nucleus collisions is smaller than the projectile mass number times that in proton-nucleus collisions. The rate of the hypernucleus production in nucleus+nucleus collisions to that in proton-nucleus collisions is mainly determined by the ratio of the Λ-particle production in both the collisions. This ratio is reasonable since experimental kaon energy spectra in Ne+Ne and $p$ +Ne collisions at 2.1 GeV/nucleon are reproduced with the present method.

Figures 8(a) and 8(b) show the double Λ-hypernucleus formation cross sections in Ne+Ne and $p$ +Ne collisions at 5 GeV/nucleon. It is seen that an increase of one Λ particle in a hypernucleus reduces the cross section by a factor of about $10^5$.

The explicit relationship between the coalescence radius $p_0$ in momentum space and the coalescence factor $S_{n\Lambda,F}$ is given by the equation

$$\frac{1}{n!}\left[\frac{4\pi}{3}p_0^3\right]^n=\left[\frac{nm_\Lambda+m_F}{m_\Lambda^n m_F}\right]^3 S_{n\Lambda,F}\ . \quad (34)$$

The $p_0$ values are shown in Table I for a few hypernuclei and are generally smaller than those of light nuclei $d$, $t$, $^3$He, $^4$He, etc.

## VII. DISCUSSION

Let us make a brief discussion of the hypernucleus production by the secondary particles. The nuclear collision produces $K^-$ mesons, whose inclusive cross section has been observed and can be basically reproduced by the model of Sec. III consistently with those of $K^+$ and Λ. (The calculated $K^-$ cross sections will be reported elsewhere.) The $K^-$ has a chance to coalesce with nuclear fragments and form a $K^-$ atom. The absorption of $K^-$ from the atomic orbits leads to hypernucleus formation via $(K^-,\pi)$ reactions.

TABLE I. Coalescence radius $p_0$.

| Hypernucleus | $p_0$ (GeV/$c$) |
|---|---|
| $^5_\Lambda$He | 0.084 |
| $^{13}_\Lambda$C | 0.108 |
| $^{17}_\Lambda$O | 0.105 |

We thus expect an additional contribution to Eq. (15)

$$R_{\Lambda F}^{(K^-)}\left[\frac{m_{K^-}+m_F}{m_{K^-}m_F}\right]^3 \times S_{K^-F}\left[\frac{\gamma}{\sigma_r}\frac{d^3\sigma(K^-)}{dk_c^3}\right]\left[\frac{\gamma}{\sigma_r}\frac{d^3\sigma^{(F)}}{dk_c^3}\right], \quad (35)$$

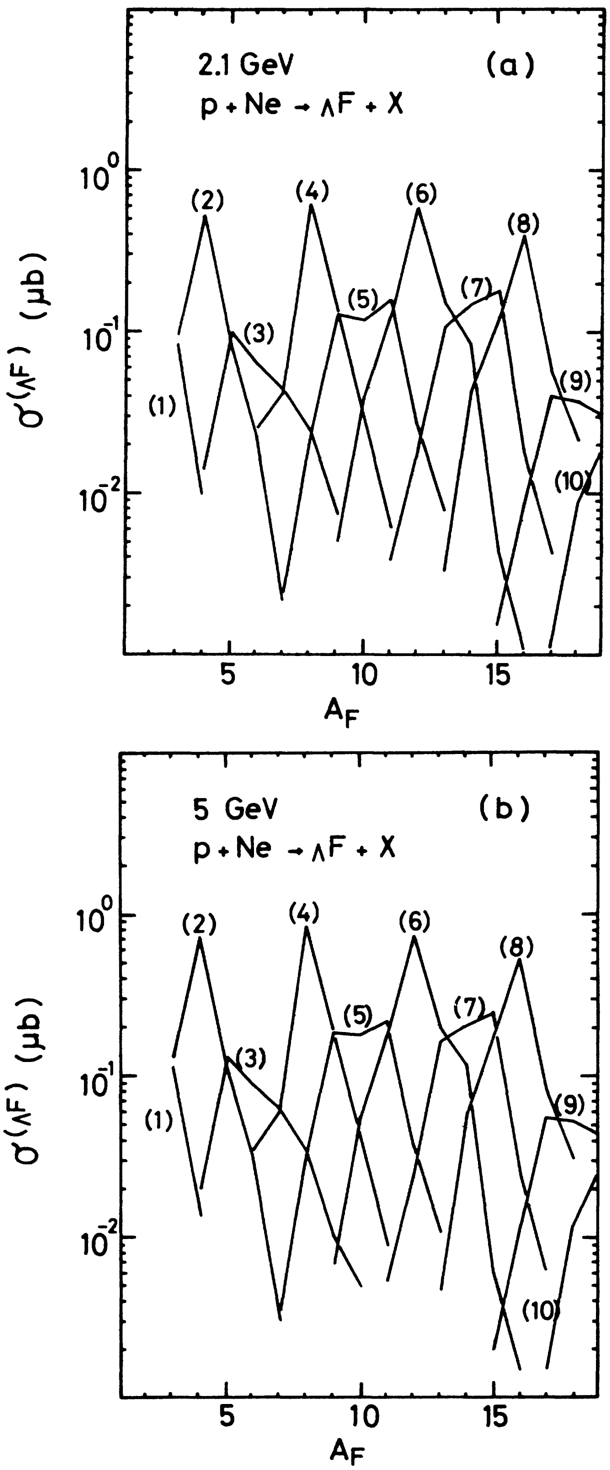


FIG. 7. The hypernucleus formation cross sections in $p$ +Ne collisions.

where $S_{K^- F}$ and $R_{\Lambda F}^{(K^-)}$ represent the coalescence factor of $K^-$ and $F$ to form a $K^-$ atom and the capture rate per $K^-$ to form the hypernucleus $(\Lambda F)$, respectively. The $K^-$ can be trapped in different $K^-$atomic orbits $\phi_{n_K l_K}$ and therefore

$$R_{\Lambda F}^{(K^-)} S_{K^- F} = \sum_{n_K l_K} R_{\Lambda F}^{(K^-)}(n_K l_K) S_{K^- F}(n_K l_K) \tag{36}$$

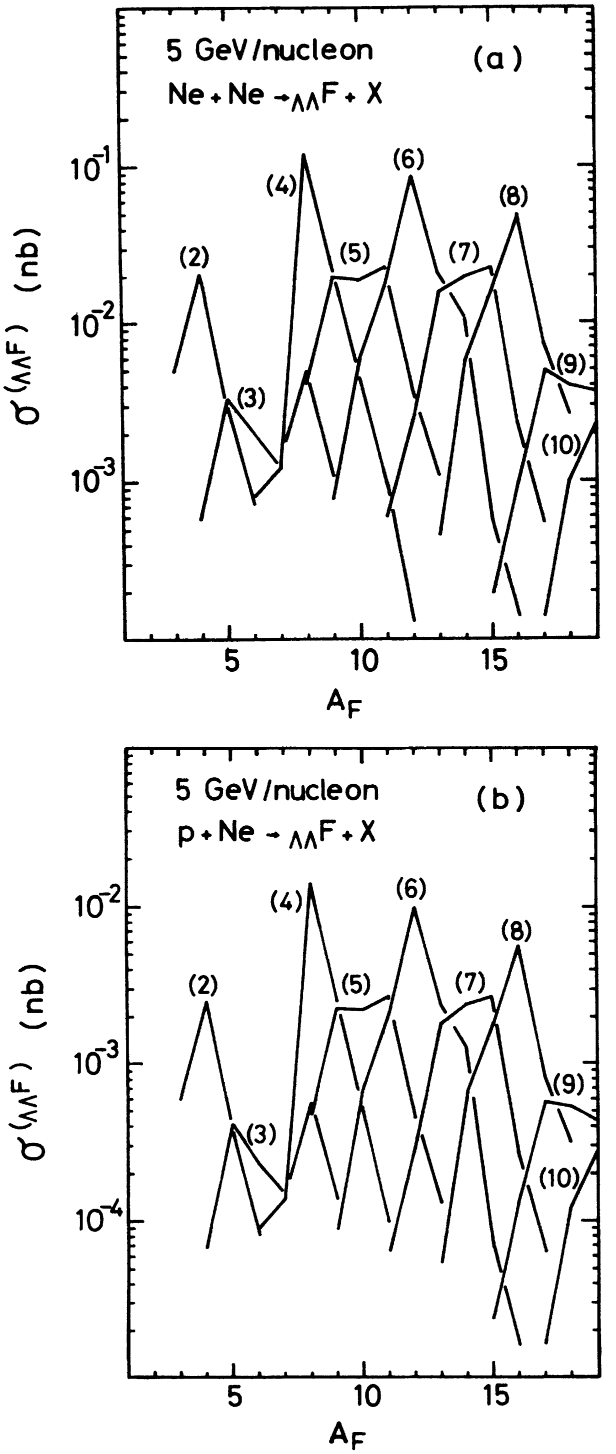


FIG. 8. The double-Λ-hypernucleus formation cross sections in Ne+Ne and $p$+Ne collisions at 5 GeV/nucleon.

with

$$S_{K^- F}(n_K l_K) = (2\pi)^3 (2l_K+1) \mathcal{S}_{K^- F}(n_K l_K) ,$$

$$\mathcal{S}_{K^- F}(n_K l_K) = \int d\mathbf{r} \, |\phi_{n_K l_K}(\mathbf{r})|^2 \xi_{K^- F}(\mathbf{r}) , \tag{37}$$

$$\xi_{K^- F}(\mathbf{r}) = \int d\mathbf{r}' D^{(K^-)}(\mathbf{r}+\mathbf{r}') D^{(F)}(\mathbf{r}') , \tag{38}$$

and

$$R_{\Lambda F}^{(K^-)}(n_K l_K) = R(K^- n \to \Lambda \pi^-) R_{\Lambda F}^{(n\to\Lambda)}(n_K l_K) + R(K^- p \to \Lambda \pi^0) R_{\Lambda F}^{(p\to\Lambda)}(n_K l_K) , \tag{39}$$

where $R(K^- N \to \Lambda\pi)$ are the branching ratios among various absorption processes, and $R_{\Lambda F}^{(n\to\Lambda)}(n_K l_K) [R_{\Lambda F}^{(p\to\Lambda)}(n_K l_K)]$ is the capture rate per $\Lambda$ for hypernucleus $(\Lambda F)$ formation through conversion of $n\,(p)$.

We estimate Eqs. (37) and (38) by using $D^{(i)}(\mathbf{r})$ of Eq. (8) with $\beta_{K^-} = \beta_\Lambda = \beta_F = 3.81$ fm (hence $\beta_{K^- F} = 5.39$ fm) and $\phi_{n_K l_K}(\mathbf{r})$ obtained by taking account of the absorption effect, the finite-size effect, etc., with the aid of the Y3/GA01 code due to Seki, Yazaki, and Masutani.[14] For $^{12}$C, the calculated $\mathcal{S}_{K^- F}(n_K l_K)$ are $1.5\times 10^{-5}$, $5.6\times 10^{-7}$, and $9.6\times 10^{-10}$ fm$^{-3}$ for $(1s)$, $(2p)$, and $(3d)$ orbits, which are to be compared with the values $\sim 10^{-3}$ fm$^{-3}$ in Fig. 5. The coalescence factor for $K^-$-atom formation is very small as expected, because $K^-$ must have almost exactly the same momentum as the fragment.

The branching ratios $R(K^- N \to \Lambda\pi)$ are known experimentally; $R(K^- n \to \Lambda\pi^-) = 0.20$ and $R(K^- p \to \Lambda\pi^0) = 0.03$. The capture rates per $\Lambda$, $R_{\Lambda F}^{(N\to\Lambda)}(n_K l_K)$, have been studied and known to be about a few percent.

Combining the above numbers, we obtain an estimate of $R_{\Lambda F}^{(K^-)} S_{K^- F}$ of Eq. (36), which is smaller at least by a factor of $10^{-3}$ than the direct coalescence of $\Lambda$ and $F$. While we can also consider the $\Sigma$-hypernucleus formation, where $R_{\Sigma F}^{(K^-)}(n_K l_K)$ defined analogously to Eq. (39) can be by 1 order larger than $R_{\Lambda F}^{(K^-)}(n_K l_K)$, we can expect that their contributions are still not significant.

The secondary pions, which are produced abundantly in nuclear collisions, may contribute to hypernuclear production through $(\pi, K^+)$ reactions. The most desirable momentum of pion is about 1 GeV/$c$ relative to the fragment. However, since the momentum distributions of pions and fragments overlap very small, we cannot expect too much contribution from this secondary process.

The effect of temporal distribution of the source functions has already been discussed in Sec. V B. It reduces the cross sections given in the figures by a factor of about 2.

In our treatment, we take account of all possible coalescences of fragments and hyperons from arbitrary origins with consideration of the time-dependent effect. Concerning the so-called impact-parameter effect, we did not explicitly take account of one to one correspondence between the production cross section and an impact-parameter value of the collisions. The production probabilities of a fragment and $\Lambda$ particle depend on the impact parameter $b$. Then the formation probability of a hypernucleus for Eq. (13) should be written as

$$P_2^{(\Lambda F)}(\mathbf{K},b)=S_{\Lambda F}P_1^{(\Lambda)}(\mathbf{k}_1,b)P_1^{(F)}(\mathbf{k}_2,b) \ . \tag{40}$$

Integrating over the impact parameter and using the Schwartz inequality, we get the following relation:

$$\langle P_2^{(\Lambda F)}(\mathbf{K})\rangle \le S_{\Lambda F}\langle P_1^{(\Lambda)}(\mathbf{k}_1)^2\rangle^{1/2}\langle P_1^{(F)}(\mathbf{k}_2)^2\rangle^{1/2} \ , \tag{41}$$

where $\langle P \rangle$ is defined by $\int_0^{b_{\max}} P(b)b\,db$ and $b_{\max}$ is the maximum value of the impact parameter. In general, an equality is not realized because the nuclear fragment and the $\Lambda$ particle have different production probabilities. In the present work, we take $S_{\Lambda F}\langle P_1^{(\Lambda)}(\mathbf{k}_1)\rangle\langle P_1^{(F)}(\mathbf{k}_2)\rangle$ as for the production probability of a hypernucleus. If $\langle P_1^{(i)}(\mathbf{k})^2\rangle^{1/2}$ is nearly equal to $\langle P_1^{(i)}(\mathbf{k})\rangle$, we can say that the calculated results give only the upper limit of the production cross sections of hypernuclei. There is need for improvement of the calculation based on the coalescence model taking into account the impact-parameter effect.

Ko[9] has also studied the formation cross section of hypernucleus in terms of the participant-spectator model taking into account the temporal distributions of the fragment and the $\Lambda$ particle and the impact-parameter dependence. Ko obtained the cross sections smaller by a factor of about $10^3$ than ours. However, it is not clear whether his model can reproduce the available experimental cross sections of nuclear fragments or not.

Recently, an experimental group in Dubna succeeded in finding five events of ${}^4_\Lambda$H production in a ${}^4$He beam (3.7 GeV/nucleon) and one event of ${}^7_\Lambda$Li in a ${}^7$Li beam (3.0 GeV/nucleon) on polyethylene target.[15] The derived cross sections are $\sim 0.2\ \mu$b for ${}^4_\Lambda$H and $\lesssim 1\ \mu$b for ${}^7_\Lambda$Li. These magnitudes are quite consistent with our predictions and seem to support the hypernuclear production mechanism adopted in the present paper.

## VIII. CONCLUSION

We have formulated the hypernucleus formation probability in nuclear collisions with a coalescence model and calculated production cross sections of hypernuclei in $p$+Ne and Ne+Ne collisions at 2.1 and 5 GeV/nucleon. The production cross sections of single-$\Lambda$ hypernucleus are of the order of $\mu$b in Ne + Ne collisions at 5 GeV/nucleon. It is found that the hypernucleus production cross sections at 5 GeV/nucleon are about a few times larger than at 2.1 GeV/nucleon and also found that the hypernucleus production cross sections in Ne + Ne collisions are a few times larger than those in $p$+Ne collisions. The production cross sections of double-$\Lambda$ hypernucleus become smaller by a factor of about $10^5$ than those of single-$\Lambda$ hypernucleus. In Ne + Ne collisions, we find that the measurement of double-$\Lambda$ hypernucleus turns out to be hard. In heavier nucleus collisions, however, number of $N+N$ collision increases nonlinearly and hence double-$\Lambda$ hypernuclei may have more chance to be produced.

We have briefly studied the hypernucleus production by the secondary particles, $K^-$ and $\pi$, produced in nuclear collisions. However, we cannot expect too much additional contribution from the processes such as $(K,\pi)$ and $(\pi,K)$.

## ACKNOWLEDGMENTS

We are grateful to Dr. H. Sato and Dr. J. Žofka for many stimulating and valuable discussions. Our thanks are also due to Dr. S. Khorozov for informing us with the recent experimental results of hypernucleus production.

## APPENDIX A

Let $\psi_{nl}$ be the harmonic-oscillator wave function of a $\Lambda$ particle in a hypernucleus. The wave function of two $\Lambda$ particles with the angular momentum $(\lambda\mu)$ is expressed as

$$\begin{aligned}\phi_{\lambda\mu}(\mathbf{r}_1,\mathbf{r}_2) &= |\,n_1l_1,n_2l_2,\lambda\mu\rangle \\ &= [\phi_{n_1l_1}(\mathbf{r}_1)\otimes\phi_{n_2l_2}(\mathbf{r}_2)]_\mu^{(\lambda)} \ .\end{aligned} \tag{A1}$$

The coordinates $\mathbf{r}_1$ and $\mathbf{r}_2$ are transformed to those between the center of mass of two $\Lambda$ particles and the nuclear fragment $F$ and between two $\Lambda$ particles, respectively. Then Eq. (A1) is rewritten as

$$\phi_{\lambda\mu}(\mathbf{R}',\mathbf{r}')=\sum |\,nl,NL,\lambda\mu\rangle\langle nl,NL,\lambda\,|\,n_1l_1,n_2l_2,\lambda\rangle \ , \tag{A2}$$

where $\langle nl,NL,\lambda\,|\,n_1l_1,n_2l_2,\lambda\rangle$ is the Talmi coefficient and

$$\mathbf{R}'=(\mathbf{r}_1+\mathbf{r}_2)/\sqrt{2}=\sqrt{2}\mathbf{R}$$

and

$$\mathbf{r}'=(\mathbf{r}_1-\mathbf{r}_2)/\sqrt{2}=\mathbf{r}/\sqrt{2} \ .$$

Total antisymmetric wave functions are given by

$$\begin{aligned}\psi_{\lambda\mu}^{\text{odd}}(\mathbf{r}',\mathbf{R}')&=\phi_{\lambda\mu}^{(-)}(\mathbf{r}',\mathbf{R}')\chi_{S=1}(\sigma_1,\sigma_2) \ , \\ \psi_{\lambda\mu}^{\text{even}}(\mathbf{r}',\mathbf{R}')&=\phi_{\lambda\mu}^{(+)}(\mathbf{r}',\mathbf{R}')\chi_{S=0}(\sigma_1,\sigma_2) \ .\end{aligned} \tag{A3}$$

The wave function $\phi_\lambda^{(\pm)}$ is defined as follows:

$$\phi_{\lambda\mu}^{(\pm)}(\mathbf{r}',\mathbf{R}')=\frac{1}{\sqrt{2}}f_\pm^{(\lambda)}\sum[1\pm(-1)^l]\,|\,nl,NL,\lambda\mu\rangle\langle nl,NL,\lambda\,|\,n_1l_1,n_2l_2,\lambda\rangle \ ,$$

where $f_\pm^{(\lambda)}=1$ for $(n_1l_1)\neq(n_2l_2)$, in the case of $(n_1l_1)=(n_2l_2)f_+^{(\lambda)}=1/\sqrt{2}$ for $\lambda$=even integer, $f_+^{(\lambda)}=0$ for $\lambda$=odd integer. Substituting the wave function (A3) into Eq. (31), we can get the expression for the coalescence factor of the double-$\Lambda$-hypernucleus formation as

$$\begin{aligned}S_{2\Lambda,F}=(\pi\beta_\Lambda)^{-3}(2\beta_F^2+\beta_\Lambda^2)^{-3/2}&\sum f_\pm^{(\lambda)^2}[1\pm(-1)^l]\langle nl,NL,\lambda\,|\,n_1l_1,n_2l_2,\lambda\rangle\langle n'l,N'l,\lambda\,|\,n_1l_1,n_2l_2,\lambda\rangle \\ &\times\int_0^\infty dr'r'^2R_{nl}(r')e^{-(r'/\beta_\Lambda)^2}R_{n'l}(r') \\ &\times\int_0^\infty dR'R'^2R_{NL}(R')e^{-R'^2/(2\beta_F+\beta_\Lambda^2)}R_{N'L}(R') \ .\end{aligned} \tag{A4}$$

[1]S. Schnetzer *et al.*, Phys. Rev. Lett. **49**, 989 (1982).
[2]J. W. Harris *et al.*, Phys. Rev. Lett. **47**, 229 (1981).
[3]A. K. Kerman and M. S. Weiss, Phys. Rev. C **8**, 408 (1973).
[4]H. Sato and K. Yazaki, Phys. Lett. **98B**, 153 (1981).
[5]F. Asai, H. Bandō, and M. Sano, Phys. Lett. **145B**, 19 (1984); in *Proceedings of the International Conference on High Energy Nuclear Physics, Balatonfüred, Hungary, 1983,* edited by J. Erö (Central Research Institute for Physics, Budapest, 1983), p. 65.
[6]M. Wakai, H. Bandō, and M. Sano, in *Proceedings of the 1986 INS International Symposium on Hypernuclear Physics, Tokyo, 1986,* edited by H. Bandō, O. Hashimoto, and K. Ogawa (Institute for Nuclear Study, University of Tokyo, Tokyo, 1986), p. 257.
[7]The density matrix $\rho$ used by Sato and Yazaki in Ref. 8 and Ko in Ref. 9 is to be understood to correspond to $\hat{\rho}$ in our formalism.
[8]H. Sato and K. Yazaki, in *Proceedings of the Hakone Seminar on High-Energy Nuclear Interactions and Properties of Dense Nuclear Matter, Hakone, 1980,* edited by K. Nakai and A. S. Goldhaber (Japan–U.S. Joint Seminar, Tokyo, 1980), p. 340.
[9]C. M. Ko, Phys. Rev. C **32**, 326 (1985).
[10]J. Knoll, Phys. Rev. C **20**, 773 (1979); Nucl. Phys. **A343**, 511 (1980).
[11]F. Asai, Nucl. Phys. **A356**, 519 (1981).
[12]J. Randrup and C. M. Ko, Nucl. Phys. **A343**, 519 (1980). J. Randrup, Phys. Lett. **99B**, 9 (1981).
[13]A. S. Gholdhaber, Phys. Lett. **53B**, 306 (1974); A. S. Goldhaber and H. H. Heckman, Ann. Rev. Nucl. Sci. **28**, 161 (1979).
[14]R. Seki, K. Yazaki and K. Masutani, Y3/TC/GA01 code in the Program Library of the Computer Center, University of Tokyo.
[15]S. Avramenko *et al.*, Dubna Report E1-87-337, 1987 (unpublished).